Effect of physical ageing on mechanical behaviour of an elastomeric glass under combined pressure and temperature

K. Vijayan, C.-L. Tang* and K. D. Pae†
High Pressure Materials Research Laboratory, Department of Mechanics and Materials Science, College of Engineering, Rutgers University, Piscataway, NJ 08855-0909, USA
(Received 1 December 1986; revised 25 June 1987; accepted 28 July 1987)

The relaxation or physical ageing behaviour of a polyurethane elastomeric glass (Solithane 113, $T_g = -20°C$ at atmospheric pressure) has been studied at various states of pressure and temperature (P,T), near and far away from the glass transition. Those (P,T) states were reached via either isobaric or isothermal paths. The relaxation behaviour of these glasses has been found to be a function of P, T and the path. The Young's modulus (E) has been determined as a function of ageing time. When all the experimental data, obtained at various (P,T) states for a specific path, were replotted in the form of log E vs. $1/P$ for an isothermal glass and log E vs. $1/T$ for an isobaric glass, all the curves appear to converge to a specific value of E. The value was chosen as E_∞, the 'near-equilibrium' modulus. The relaxation behaviour was analysed by a parameter

$$\delta^E = \frac{E_\infty - E(P,T,t)}{E_\infty}$$

When $\delta^E \simeq 1$ is used to define a glass transition, the pressure-dependent glass transition lines for isobaric glasses are found to be entirely different from those for isothermal glasses. This may be the result of the pressure rate and temperature rate used. The non-equilibrium behaviour of E of the glass was analysed by an equation analogous to Kovac's equation for the kinetics of relaxation, namely

$$\frac{-\mathrm{d}\delta^E(P,T,t)}{\mathrm{d}t} = \frac{\delta^E(P,T,t)}{\tau(P,T,\delta^E)}$$

where $\delta^E(P,T)$ is the relative departure of $E(P,T,t)$ from E_∞. In general, the isobaric glasses at a specific state (P,T) relaxed faster, relatively, than isothermal glasses for the experimental conditions of heating rate or pressurization rate.

(Keywords: physical ageing; high pressure; elastomeric glass; isobaric and isothermal glasses; Young's modulus)

INTRODUCTION

Attention has been focused recently on the properties of glasses that have been prepared from the melt under elevated pressure[1-11]. Because of the strong dependence of T_g on pressure, glasses made in this manner actually have been vitrified at different temperatures. These glasses are characterized by reduced volume and increased population of high-energy bonds[3-7]. The studies of pressure-densified glasses were carried out by most workers at atmospheric pressure after pressure was released. Those glasses are highly unstable and undergo 'memory behaviour' of structural relaxation with time[12]. Theoretical equations of state have been developed to describe the pressure–volume–temperature relations of polymers[13-15]. The theories are mostly applicable to the liquid state since there is a true thermodynamic state characterized by a single surface in P–V–T space. The same is not true for the glassy state where the volume depends on the glass formation pressure as well as on ambient pressure, temperature and the rate at which the glass is formed[14,16-19]. Pressure increases T_g anywhere from 10 to 35°C per kilobar[20,21]. Thermodynamic theories are developed on the assumption that T_g is or reflects a true second-order thermodynamic transition.

The nonlinear dependence of relaxation time on the structural change of glass has been approached phenomenologically by Moynihan and coworkers[22,23]. Moynihan's model is modified to include hydrostatic pressure on the temperature dependence of relaxation time[24]. The effect of hydrostatic pressure on relaxation of polymer glass is also analysed statistically[25,26]. Based on molecular dynamics, predictions are made for volume recovery in polymer glasses[27]. High-pressure-jump experiments on volume relaxation of polystyrene have been reported and compared with temperature-jump results[28]. The dependence of log τ on pressure is linear within the limited pressure range studied (about 0.6 kbar). The WLF equation has been modified to describe the time–temperature–pressure superposition of stress-relaxation data under a combined state of pressure and temperature[29-31]. The modified expression, originally developed from tensile stress-relaxation data,

---

* On leave from China Textile University, Shanghai, People's Republic of China

† To whom correspondence should be addressed

0032-3861/88/030396-09$03.00

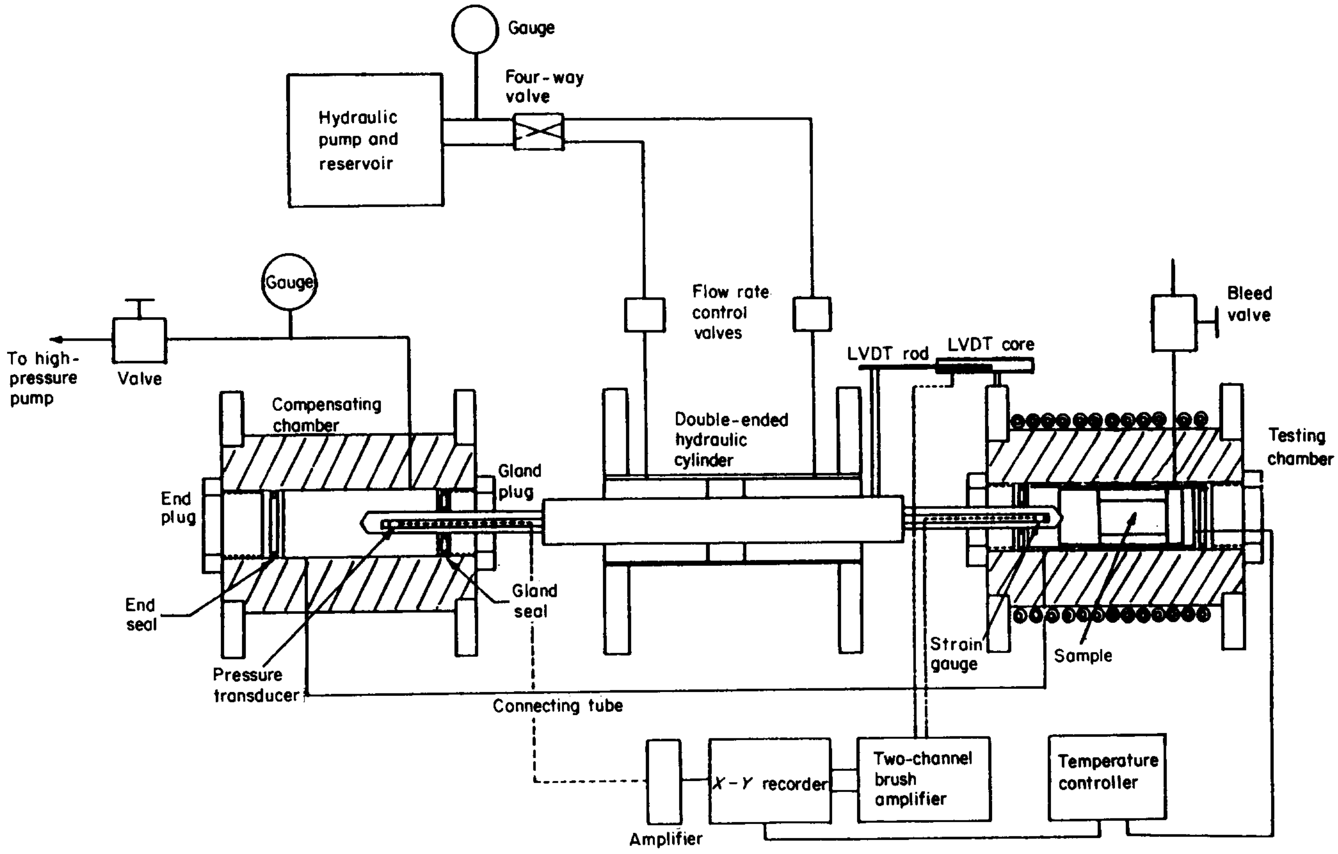

Figure 1 Schematic diagram of the high-pressure stress–strain testing apparatus

has been applied to shear stress-relaxation data[32].

In this paper, the results of a study on the physical ageing behaviour of a polyurethane elastomeric glass at various pressures and temperatures, near and far from the glass transition, are presented. The samples were given two distinct thermodynamic histories, namely isobaric or isothermal paths, in arriving at the various states of pressure and temperature. While the glasses were relaxing, an instantaneous compressive loading was applied to obtain the stress–strain response. The Young's modulus (E), which was determined by drawing a tangent to the linear elastic curve through the origin of the stress–strain curves, was used to monitor the ageing behaviour.

MATERIAL

Solithane 113 is a commercially available urethane elastomer (Thiokol Chemical Co.). It is formed from the reaction of a resin and a catalyst. The resin is a prepolymer formed by extending castor oil with tolylene diisocyanate. No specific chemical composition of the polyurethane elastomer is available as the manufacturer kept the information proprietary. The catalyst also consists essentially of castor oil[33,34]. By varying the amounts of catalyst and resin, the properties of the resulting elastomer can be greatly varied. In the present study only the equal-volume (50/50) composition was examined. For this composition the specific volume at atmospheric pressure and room temperature was $0.97\,\mathrm{cm^3\,g^{-1}}$ and at atmospheric pressure it has a glass transition temperature of -20°C. On the basis of swelling measurements the average molecular weight between crosslinks was determined[34] to be about $2000\,\mathrm{g\,mol^{-1}}$.

EXPERIMENTAL

The schematic diagram of the high-pressure testing apparatus is shown in *Figure 1*. The apparatus consists of two thick-walled cylindrical pressure vessels, one for testing and the other for pressure compensations. A double-ended hydraulic cylinder situated between them has two protruding pistons, which are projected into the pressure vessels. The pistons contain a full-bridged strain gauge, mounted inside the $\frac{3}{16}$ inch (5 mm) cylindrical cavity and near one end of the pistons, which monitors the applied load and pressure, respectively. A linear variable differential transformer measures displacement of the specimen. Silicone oil (Dow Corning 200 fluid) is used as the pressure medium. The test vessel is designed to accommodate an internal furnace and an external cooling coil. The apparatus is capable of testing a sample at pressures to 7 kbar and temperatures from -100 to $+100$°C. The rate of compressive loading used for this series of tests is $0.02\,\mathrm{inch\,min^{-1}}$ ($0.5\,\mathrm{mm\,min^{-1}}$).

The time-independent mechanical behaviour of Solithane 113 has been determined previously in the liquid and glassy states at high pressures up to 5.0 kbar and room temperature (20°C) by Questad *et al.*[35,36] A three orders of magnitude increase of Young's modulus (E) within this pressure range at room temperature was observed. In this study, Solithane glass is obtained as a function of pressure and temperature (P,T), path by which these states were arrived at, and ageing time. Compressive stress–strain tests were performed and E was obtained by drawing a tangent line to the linear elastic curve through the origin.

An elastomeric glass at a given specific glassy state (P,T) would show a characteristic mechanical behaviour

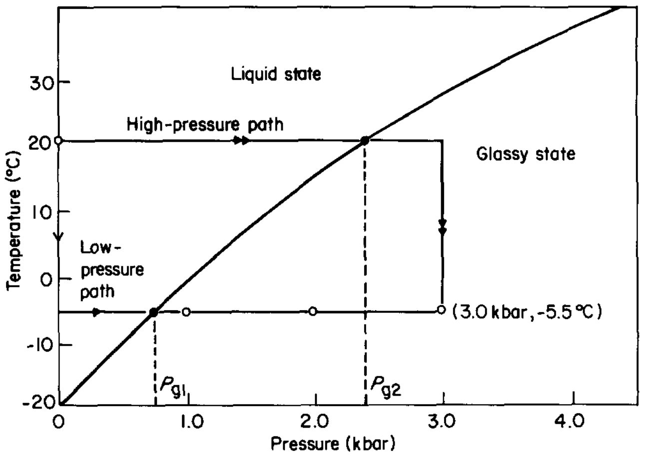

Figure 2 Schematic path profile to reach the experimental state in the P–T plane

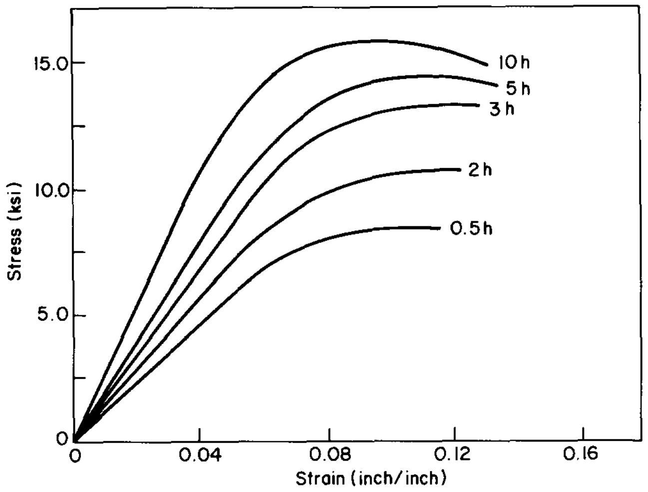

Figure 3 Ageing time dependence of compressive stress–strain curves at the state ($P=3.0$ kbar, $T=-5.5$°C) reached by high-pressure path

of that state and would undergo relaxation as a function of ageing time. Initially the experiments were designed based on the scheme shown in *Figure 2*, where the phase diagram of Solithane was obtained from the experimental conditions described in earlier work[36]. Since T_g is the manifestation of kinetic conditions, the phase diagram given in *Figure 2* is a non-equilibrium one.

As shown in *Figure 2*, the glassy state ($P=3.0$ kbar, $T=-5.5$°C) is reached by two paths. By the high-pressure path, a liquid (rubbery) sample is, first, pressurized from atmospheric pressure to 3.0 kbar and then the temperature is lowered from 20 to -5.5°C. By the low-pressure path, the temperature of the rubbery sample is first lowered from room temperature to -5.5°C and then the pressure is raised to 3.0 kbar. In all cases of experiments reported in this work, the pressurization rate (p) of 0.25 kbar min^{-1} and the cooling rate (q) of 0.5°C min^{-1} are used to reach the (P,T) state. The glass sample formed by the high-pressure path is aged for 0.5 h at the (P,T) state and an instantaneous compressive load is applied to get the stress–strain curve. In another test, a new liquid sample, similarly brought to the same (P,T) state, is aged for 2.0 h and then tested in compression. A series of samples were subsequently tested with longer ageing time. The mechanical response of the glass formed by the low-pressure path is obtained for various ageing times in a similar way as that obtained for the high-pressure path. It is emphasized here that, in any set of ageing experiments, we always start with a new rubbery sample. Thus the chronology of glass history in ageing experiments is preserved without ambiguity[37].

RESULTS

The compressive stress–strain curves of the glasses obtained at various ageing times for high- and low-pressure paths are shown in *Figures 3* and *4*, respectively. The stress–strain curves clearly show the path dependence as the 0.5 h curve for the high-pressure path is much lower in the elastic modulus (E), yield strength (σ) and stored elastic energy (e) than those of the low-pressure path curve. The stress–strain curves are shifted upwards as functions of ageing time, exhibiting increased E, σ and e. *Figure 5* shows the ageing time dependence of E[38]. The E of the high-pressure path samples crosses over the low-pressure path curve, indicating that the relaxation processes of the glassy state by the two paths are entirely different, that is, the high-pressure path glass relaxes faster than the low-pressure path glass.

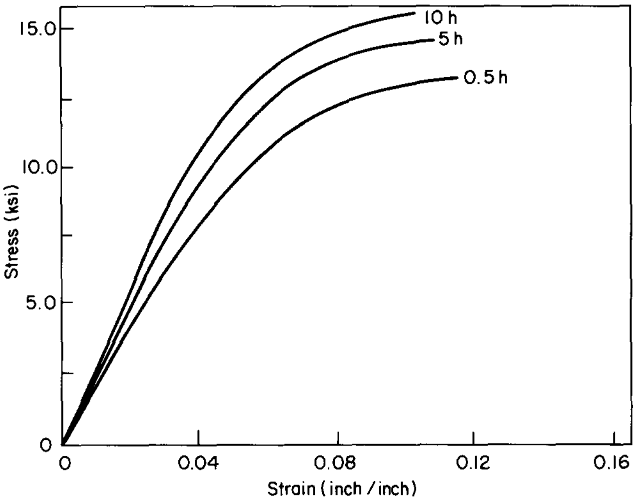

Figure 4 Ageing time dependence of compressive stress–strain curves at the state ($P=3.0$ kbar, $T=-5.5$°C) reached by low-pressure path

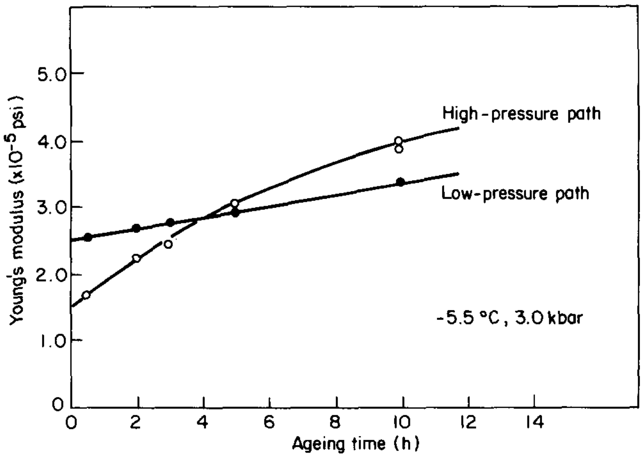

Figure 5 Ageing time dependence of Young's modulus by two different paths

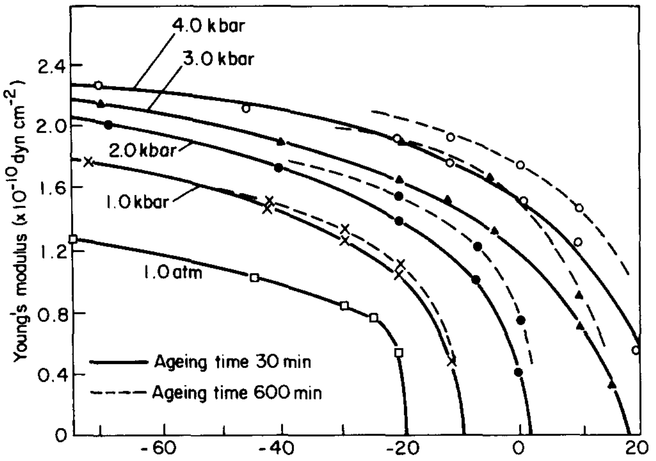

Figure 6 Young's modulus of isobaric glasses at various states

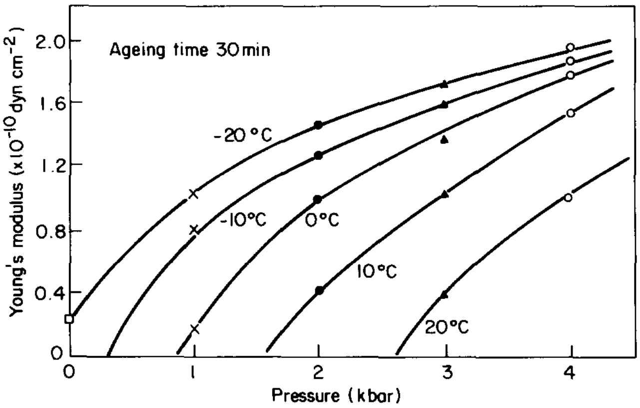

Figure 7 Young's modulus of isothermal glasses at various states

Figure 6 shows the values of E of the glasses formed by isobaric paths (isobaric glasses) at various states (P,T) for an ageing time of 30 min. *Figure 7* shows the same for the glasses by isothermal paths (isothermal glasses). The test procedure followed for an isobaric glass at 3.0 kbar and 4.5°C, for example, was that a rubbery sample at room temperature was pressurized first to 3.0 kbar and then the temperature was lowered to 4.5°C. Once the state $(P = 3.0\,\text{kbar},\ T = 4.5°\text{C})$ was reached, it was aged for 30 min and loaded immediately for the elastic response. Annealing, if any, during the travel time to reach various states has been ignored.

For isobaric glasses, as shown in *Figure 6*, the E at 30 min, as well as at 600 min ageing, increases but with a decreasing rate with decreasing temperature. For example, the E of the atmospheric glass, the glass being formed under atmospheric pressure and at -20°C, rises very rapidly with decreasing temperature of ageing in the neighbourhood of the transition temperature but the rapid rise diminishes below about -25°C. By increasing the glass formation pressure from 1 bar to 1, 2, 3 and 4 kbar, it can be observed that the rate of increase of the modulus with decreasing temperature of ageing slows with pressure. A similar observation can be made on isothermal glasses; that is, the rate of increase of E decreases with decreasing temperature of ageing (*Figure 7*).

E is, therefore, dependent on pressure, temperature, ageing time and path (j) by which the state is reached:

$$E^j = E^j(P,T,t) \tag{1}$$

Figures 6 and *7* are replotted in the form of log E vs. $1/T$, as shown in *Figure 8* for isobaric glasses, and log E vs. $1/P$, as shown in *Figure 9* for isothermal glasses. *Figures 8* and *9* show extrapolation of E to very low temperature or very high pressure, respectively, for isobaric or isothermal glasses. To obtain the convergence point, we fit each subset of experimental data, such as the 2.0 kbar glass, in a polynomial form

$$y = A + Bx + Cx^2 + Dx^3 + \ldots$$

and solve a set of equations for isobaric or isothermal glasses simultaneously. It was realized, however, that this procedure had drawbacks. The reason for the drawbacks was that E rose abruptly near the transition in all glasses and thus the selected coefficients, being sensitive, did not produce convergence to a point that was required. A different approach was adopted. Each set of the data was fitted by two separate equations, namely

$$y = A + Bx + Cx^2$$

or

$$y = A + Bx + Cx^2 + Dx^3$$

near the transition and

$$y = A + Bx$$

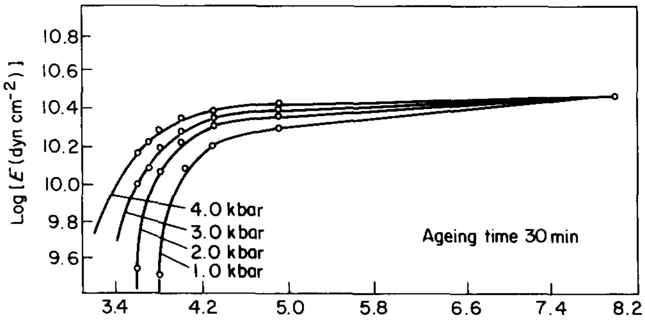

Figure 8 Log E vs. $1/T$ for isobaric glasses

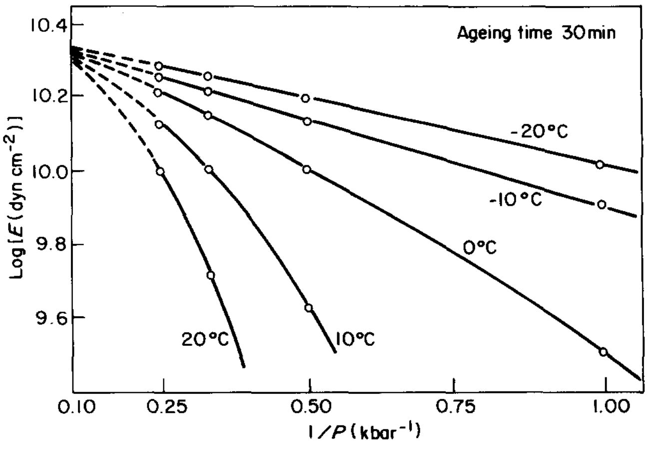

Figure 9 Log E vs. $1/P$ for isothermal glasses

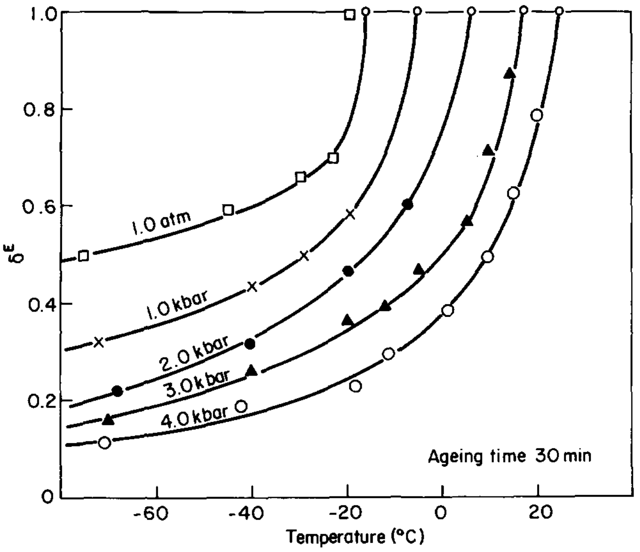

Figure 10 δ^E at various states for isobaric glasses

far away from transition. The total ideal error square for 'i' experimental points of a particular set of the data would be:

$$D = \sum_i [f_i(x,y)]^2 \tag{2}$$

where

$$f_i = y - A_i - B_ix \tag{3a}$$

$$f_i = y - A_i - B_ix - C_ix^2 \tag{3b}$$

$$f_i = y - A_i - B_ix - C_ix^2 - D_ix^3 \tag{3c}$$

The least mean square was obtained by differentiating (2) and equating it to zero:

$$\frac{\partial D(x,y)}{\partial x} = 0 \tag{4a}$$

$$\frac{\partial D(x,y)}{\partial y} = 0 \tag{4b}$$

By substituting (3b) into (2) and differentiating, one obtains:

$$\sum_i [2C_i^2x^3 + 3B_iC_ix^2 - 2C_ixy + (2A_iC_iB_i^2)x - B_iy + A_iB_i] = 0 \tag{5a}$$

and

$$\sum_i [y - A_i - B_ix - C_ix^2] = 0 \tag{5b}$$

which are regrouped, respectively, as:

$$Oy + Px + Sx^2 + Txy + Ux^3 = Q \tag{6a}$$

$$Ly_l + Mx + Rx^2 = N \tag{6b}$$

By means of iteration, y and y_l were calculated until they match. The matching point ($x^* = 1/T$ or $1/P$, $y^* = E$) will be the convergence point where the least mean square of all lines would be zero. The computer program for the above calculation can be found in ref. 39.

It was determined that E converged to a point at $T = -145$°C for the isobaric glasses and to a point at $P = 9.7$ kbar for the isothermal glasses. The extrapolated E values were 2.82×10^{10} dyn cm^{-2} for the isobaric glasses and 2.24×10^{10} dyn cm^{-2} for the isothermal glasses. This perhaps means that these values are yet to reach the true equilibrium value. Because of different glass formation history, two distinct values of E were produced. However, the higher value ($E_\infty = 2.82 \times 10^{10}$ dyn cm^{-2}) is assumed to be a 'pseudo- or near-equilibrium' value (E_∞) for the purpose of analysing the kinetics of ageing, using a new definition:

$$\delta^E = \frac{E_\infty - E(P,T,t)}{E_\infty} \tag{7}$$

This is analogous to Kovac's equation

$$\delta = \frac{V(T,t) - V_\infty}{V_\infty}$$

where V_∞ is the equilibrium volume.

Figures 10 and *11* show, respectively, the replotting of the experimental data in the form of δ^E vs. T of *Figure 6* and P of *Figure 7*. Since the value of δ^E at $T_g(P)$ is approximately 0.99, the new $T_g(P)$ values were picked from $\delta^E = 1$ in *Figures 10* and *11*. The values, which best represent the experimental conditions, are plotted in *Figure 12*. These curves are manifestations of P, p, T, q and path history of the samples. This new P–T phase diagram was used in determining the location of various (P,T) states at which the relaxation studies are to be carried out.

Now the results of the longer-time relaxation experiments on Solithane glasses are presented. The ageing effect of Solithane 113 is studied at different (P,T) states for the various glasses being formed by isobaric or isothermal paths according to the schemes given in *Figures 13* and *14*. The transition lines from *Figure 12* are

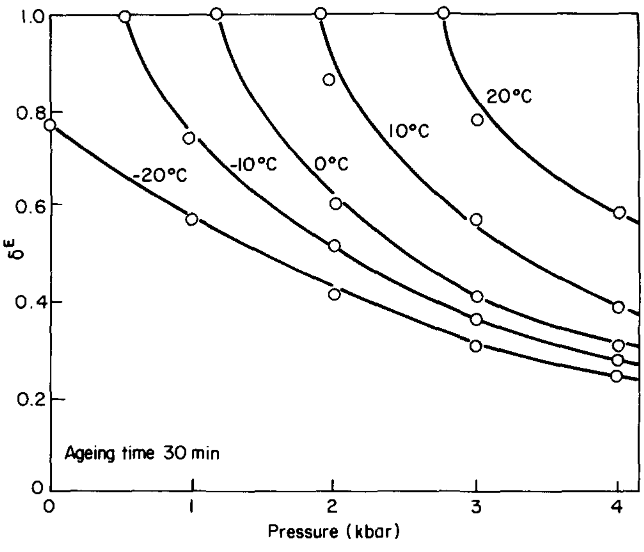

Figure 11 δ^E at various states for isothermal glasses

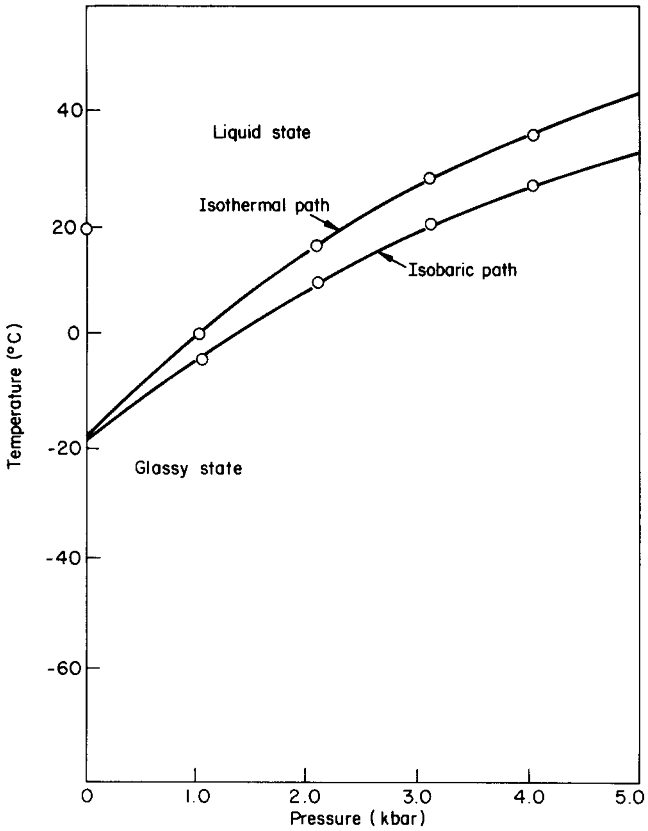

Figure 12 Path dependence of glass transition

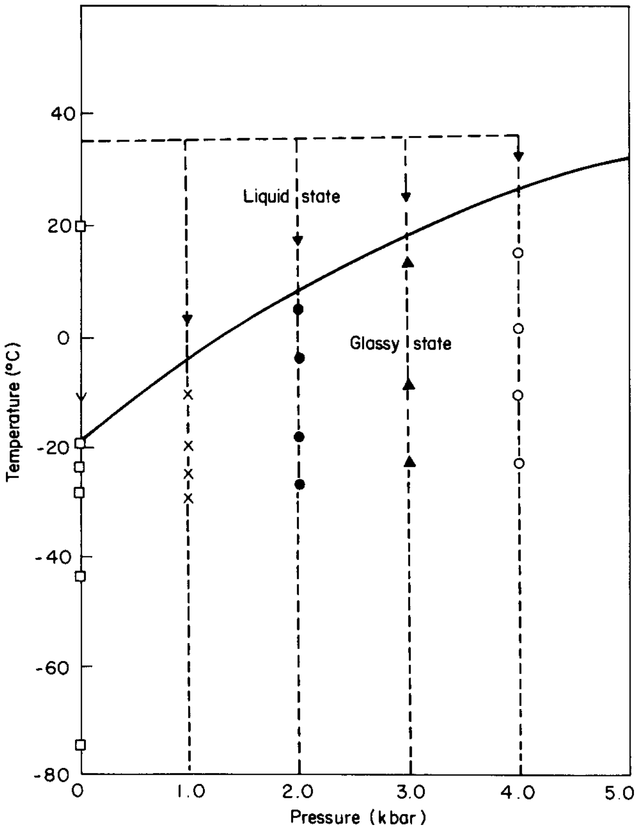

Figure 13 Path profile to reach the experimental state (*P*,*T*) for isobaric glasses

used in *Figures 13* and *14*. To form a specific glass by the isobaric path, the liquid sample is heated to 35.0°C from room temperature, subjected to different pressure levels, and cooled immediately with pressure 1.0, 2.0, 3.0 and 4.0 kbar, respectively. The specific isobaric glass formed this way is cooled to a specific (*P*,*T*) state, aged for a specific time and then loaded for the elastic response. The test is repeated for various (*P*,*T*) states at various ageing times with a new sample for each test and a typical ageing behaviour of 4 kbar glass is shown in *Figure 15*. The relaxation experiments on the isothermal glasses are carried out at various states (*P*,*T*) as marked in *Figure 14* for which the new transition curve from *Figure 12* was also used.

Figures 15 and *16* show typical relaxation behaviour of isobaric and isothermal glasses, respectively, at different (*P*,*T*) states. As shown in *Figure 15*, the *E* of 4 kbar glass increased at different rates, depending upon its temperature. Samples were tested at −10, 0, 4.5 and 15°C, but all at the same pressure, 4 kbar. The percentage

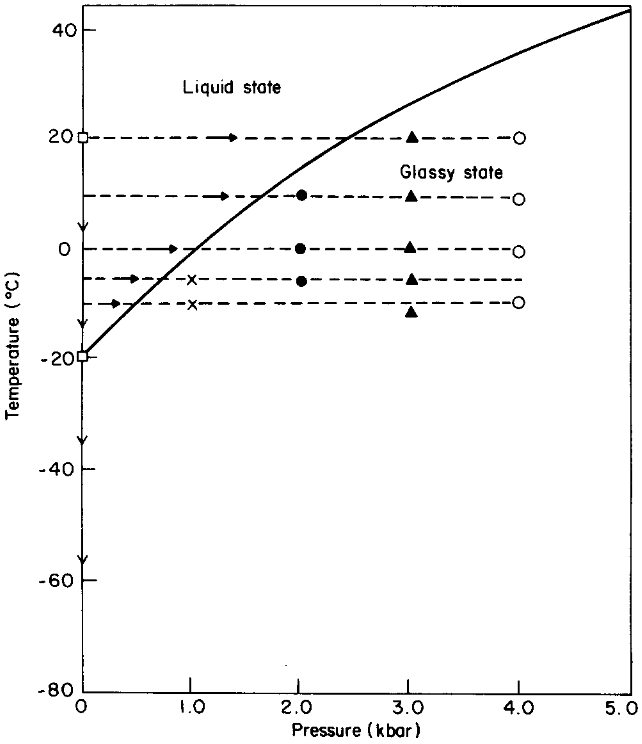

Figure 14 Path profile to reach the experimental state (*P*,*T*) for isothermal glasses

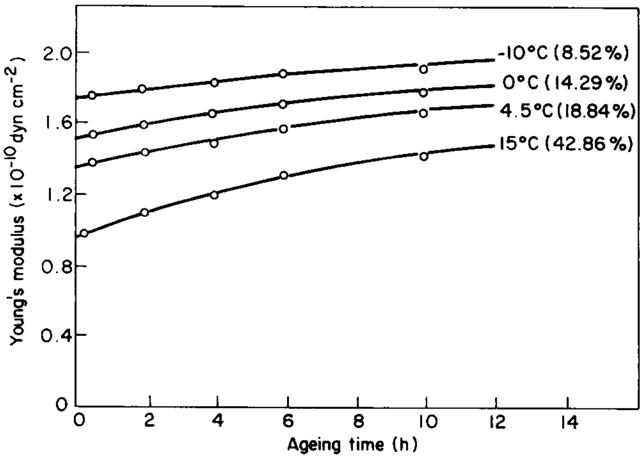

Figure 15 Ageing time dependence of Young's modulus for 4 kbar isobaric glasses

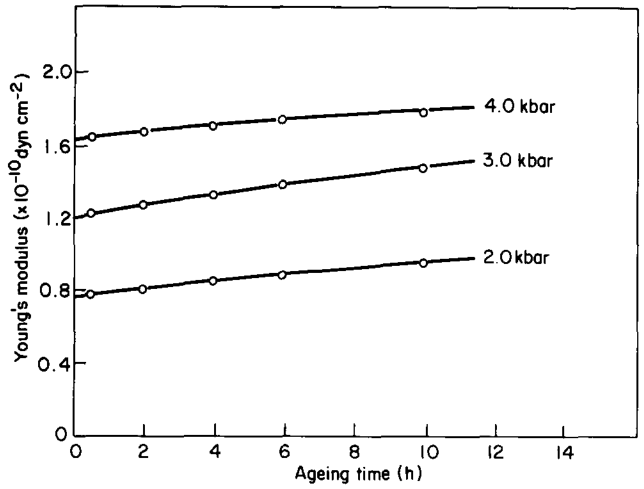

Figure 16 Ageing time dependence of Young's modulus for 4.5°C isothermal glasses

increase of E at 10 h ageing was indicated in the figure. The E increased at a very slow rate when temperature was either very close to or very far away from T_g ($=24$°C) at 4 kbar. Thus, the maximum increase of E occurred at an intermediate temperature, namely 15°C. The E of 4.5°C isothermal glass (glass formed at 1.4 kbar) increased at various rates, depending upon the ageing pressure (*Figure 16*). The maximum percentage increase of E in 10 h of ageing occurs at an intermediate pressure of 3 kbar. The increase at 2 kbar, which is near P_g, is less and at 4 kbar, which is farther away from P_g, it is also less than that at 3 kbar, where P_g is the pressure at which the glass transition occurs for that experimental temperature.

DISCUSSION

The experimental results show that E increased with ageing time and the increase depended upon the (P,T) state at which the ageing occurred and the path (isobaric or isothermal) by which the (P,T) state was arrived at. It can be shown that the change in E is directly proportional to the change in volume or δ due to physical ageing, provided that the instantaneous compressive response is linear elastic, as:

$$\delta = A^j(P,T)\left(\frac{1}{E(t)} - \frac{1}{E_\infty(P,T)}\right)$$

where $\delta = (V - V_\infty)/V_\infty$, the proportionality function A being a function of P, T, the path (j), the Young's modulus $E(t)$ at ageing time t, and the equilibrium Young's modulus $E_\infty(P,T)$. It should be obvious that physical ageing depends on the (P,T) state at which ageing is carried out. If a (P,T) state is in the neighbourhood of the glass transition (T_g) for that given P, or far away from T_g, the ageing would be slow. At an intermediate (P,T) state, the ageing is rather fast. The path dependence is, of course, due to different glasses (ξ glass), which were formed at different pressure with the pressure rates (p) and temperature rates (q) used.

The plot of log E vs. $1/P$ for isothermal glasses (*Figure 9*) shows that all the curves appear, when extrapolated, to converge to a point. The value of pressure at this point is approximately 10 kbar and the value of E is 2.24×10^{10} dyn cm^{-2}. The E for isobaric glasses similarly obtained from the plot of log E vs. $1/T$ is about 2.82×10^{10} dyn cm^{-2}, which occurred at $T = -145$°C. Under these conditions, namely $P \simeq 10$ kbar or $T = -145$°C, any molecular motion would be very limited for Solithane elastomer; therefore $E = 2.82 \times 10^{10}$ dyn cm^{-2} should be very close to the equilibrium value.

The concept of equilibrium modulus is also necessary to establish the kinetics of relaxation. Analogous to the KAHR model[40], the recovery of glasses at a given state of pressure and temperature can be analysed in terms of a very sensitive rate parameter, called τ_{eff} and defined by:

$$\tau^{-1}_{\mathrm{eff},P,T} = -\frac{1}{\delta^E}\frac{\mathrm{d}\delta^E}{\mathrm{d}t}\bigg|_{P,T} > 0 \qquad (8)$$

We may calculate the effective relaxation time based on this equation for all relaxation data of different states for both glasses in order to obtain log τ_{eff} vs. δ^E plots. *Figures 17* and *18* show some of the plots for both isobaric and isothermal glasses.

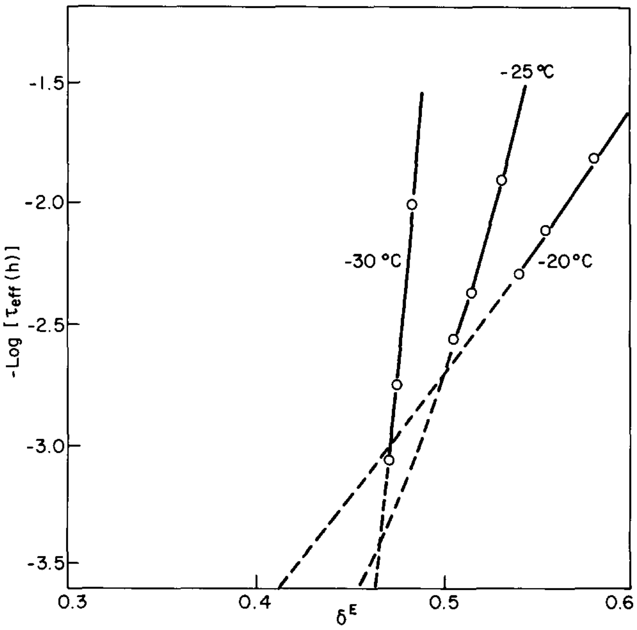

Figure 17 Log τ_{eff} vs. δ^E for 1.0 kbar isobaric glass

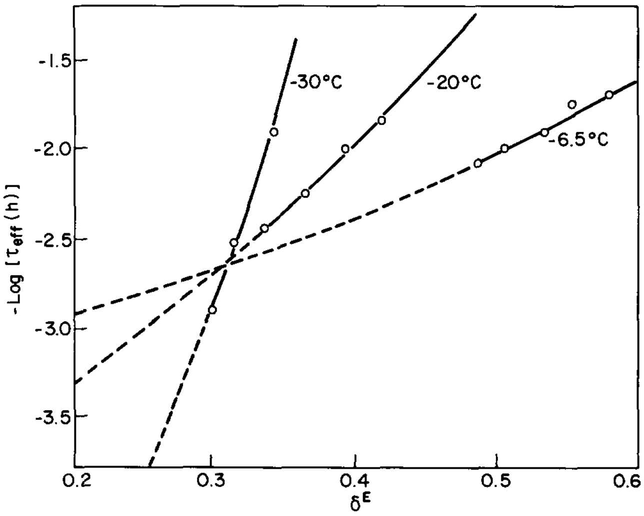

Figure 18 Log τ_{eff} vs. δ^E for 2.0 kbar isobaric glass

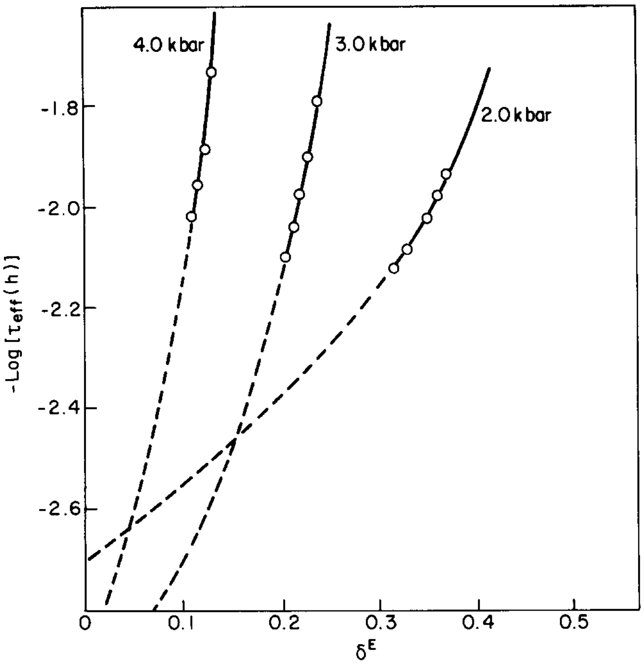

Figure 19 Log τ_{eff} vs. δ^E for -15.0°C isothermal glass

Figure 17 shows the log τ_{eff} plot for 1.0 kbar isobaric glass. The full lines are drawn based on the experimental data. Using this time window we look at the complete relaxation process up to equilibrium through the broken lines, which are extrapolated from the full lines. The intersection of a broken line with the ordinate ($\delta^E = 0$) gives the time that would be required to reach equilibrium for a particular (P,T). By decreasing the temperature from -20.0 to -30.0°C, the slope of these curves becomes higher, leading to longer relaxation time to reach equilibrium.

Figure 18 shows the same trend that, by decreasing the temperature from -6.5 to -30.0°C, a longer relaxation time is needed to reach equilibrium for the 2.0 kbar isobaric glass. But the magnitudes of the equilibrium relaxation times for the 2.0 kbar isobaric glass at different temperatures studied are relatively shorter than those of the 1.0 kbar isobaric glass at different temperatures. For example, at -20.0°C, it takes $10^{2.45}$ h to reach equilibrium for a 2.0 kbar isobaric glass, whereas it takes $10^{33.4}$ h for a 1.0 kbar isobaric glass. In short, by decreasing the temperature, an isobaric glass takes a longer time to reach equilibrium. This is expected because the mobility of the polymer chains is restricted more and more at lower temperature. By increasing the glass formation pressure, the relaxation of isobaric glass is faster in reaching equilibrium. This is reasonable because, by increasing the glass formation pressure at relatively high temperatures, more and more high-energy conformations are frozen-in[8,11] and they relax faster than the frozen conformations of the glass formed at low pressure and temperature.

Figure 19 shows the relaxation behaviour of isothermal glass formed at -15°C at different pressures. From the slopes of all these curves, it appears that the effective relaxation time of the atmospheric pressure glass at -15°C increases with pressure. This is true for cases of low glass formation pressures and is in accordance with the observation by others[28]. Summarizing, at glass formation pressure of low magnitude, the effective relaxation time increases with increase of pressure[28]. However, it was observed that, at elevated glass formation pressure and consequently high temperature, the effective relaxation time decreases with increase of pressure. This reverse phenomenon appears to occur at between -6.5°C ($P_g = 0.7$ kbar) and $+4.5$°C ($P_g = 1.4$ kbar).

ACKNOWLEDGEMENT

The authors are grateful to the Office of Naval Research (Contract N00016-82-K-0608) for the financial support to carry out this work.

REFERENCES

1 Kimmel, R. M. and Uhlmann, D. R. *J. Appl. Phys.* 1970, **41**, 2917
2 Kimmel, R. M. and Uhlmann, D. R. *J. Appl. Phys.* 1971, **42**, 4917
3 Dale, W. C. and Rogers, C. E. *J. Appl. Polym. Sci.* 1972, **16**, 21
4 Yourtee, Y. B. and Copper, S. L. *J. Appl. Polym. Sci.* 1974, **18**, 897
5 Weitz, A. and Wunderlich, B. *J. Polym. Sci., Polym. Phys. Edn.* 1974, **12**, 2473
6 Wetton, R. E. and Moneypenny, H. G. *Br. Polym. J.* 1975, **7**, 51
7 Brown, I. G., Wetton, R. E., Richardson, M. J. and Savill, N. J. *Polymer* 1978, **19**, 659
8 Prest, W. M., Jr, O'Reilly, J. M., Roberts, F. J., Jr and Mosher, R. A. *ACS Polym. Prepr.* 1980, **21**, 12
9 O'Reilly, J. M. and Mosher, R. A. *J. Appl. Phys.* 1980, **51**(10), 5137
10 Prest, W. M., Jr and Roberts, F. J., Jr *Ann. N.Y. Acad. Sci.* 1981, **371**, 67
11 O'Reilly, J. M. and Mosher, R. A. *J. Polym. Sci., Polym. Lett. Edn.* 1979, **17**, 731
12 Roe, R. J., Song, H. H. and Curro, J. J. *Bull. Am. Phys. Soc.* 1984, **29**(3), 325
13 Simha, R. and Somcynsky, T. *Macromolecules* 1969, **2**, 342
14 Quach, A. and Simha, R. *J. Appl. Phys.* 1974, **42**, 4592
15 Haoki, M., Mori, H. and Owada, A. *Macromolecules* 1981, **14**, 1567
16 McKinney, J. E. and Goldstein, M. *J. Res. Nat. Bur. Stand.* 1974, **78A**, 331
17 Gee, G. *Polymer* 1966, **7**, 177
18 McKinney, J. E. and Belcher, H. V. *J. Res. Nat. Bur. Stand.* 1963, **67A**, 43
19 Oels, H. J. and Rehage, G. *Macromolecules* 1977, **10**, 1036
20 Bhateja, S. K. and Pae, K. D. *J. Macromol. Sci.–Rev. Macromol. Chem.* 1975, **C13**(1), 77
21 Warfield, R. W. *Polym. Eng. Sci.* 1966, **6**, 2
22 Moynihan, C. T., Boesch, L. P. and LaBerge, N. L. *Phys. Chem. Glasses* 1973, **14**, 122
23 DeBolt, M. A., Easteal, A. J., Macedo, P. B. and Moynihan, C. T. *J. Am. Ceram. Soc.* 1976, **59**, 16
24 Hodge, I. M. *Bull. Am. Phys. Soc.* 1984, **29**, 327
25 Chow, T. S. *Polym. Eng. Sci.* 1984, **24**, 11
26 Chow, T. S. *Polym. Commun.* 1983, **24**, 77
27 Robertson, R. E., Simha, R. and Curro, J. G. *Bull. Am. Phys. Soc.* 1984, **29**(3), 326
28 O'Reilly, J. M., Tribone, J. J. and Greener, J. *Bull. Am. Phys. Soc.* 1984, **29**(3), 326
29 Fillers, R. W. and Tschoegl, N. W. *Trans. Soc. Rheol.* 1977, **21**(1), 51
30 Moonan, W. K. and Tschoegl, N. W. *Macromolecules* 1983, **16**, 55
31 Moonan, W. K. and Tschoegl, N. W. *Int. J. Polym. Mater.* 1984, **10**, 199
32 Moonan, W. K. and Tschoegl, N. W. *J. Polym. Sci., Polym. Phys. Edn.* 1985, **23**, 623
33 Knauss, W. G. *Int. J. Fract. Mech.* 1967, **3**, 267
34 Knauss, W. G. and Muller, H. K. 'The Mechanical Characterization of Solithane 113', Technical Report Galcit SM 67–8, California Institute of Technology, 1968
35 Questad, D. L., Pae, K. D., Scheinbeim, J. I. and Newman, B. A. *J. Appl. Phys.* 1981, **52**(10), 5977
36 Questad, D. L. 'Pressure Effect on Mechanical Properties of

Solithane', Ph.D. Thesis, Rutgers University, New Brunswick, NJ, 1981

37 Struik, L. C. E. 'Physical Aging in Amorphous Polymers and Other Materials', Elsevier, New York, 1978

38 Pae, K. D., Vijayan, K. and Tang, C. L. 'Proc. Int. Conf. on Deformation, Yield and Fracture of Polymers', Rubber and Plastics Institute, London, p. 3.1, 1985

39 Vijayan, K. 'The Effect of Aging on Mechanical Behavior of an Elastomeric Glass under Combined Pressure and Temperature', Ph.D. Thesis, Rutgers University, New Brunswick, NJ, 1986

40 Kovacs, A. J., Aklonis, J. J., Hutchinson, J. M. and Ramos, A. R. *J. Polym. Sci., Polym. Phys. Edn.* 1979, **17**, 1097